An Experimental Study on the Improvement of Aerodynamic Characteristics of Lifting Body Configuration by Active Flow Control Method

Tsuchiya, Shigeki
Department of Aeronautics and Astronautics, Kyushu University

Aso, Shigeru
Department of Aeronautics and Astronautics, Kyushu University

Tani, Yasuhiro
Department of Aeronautics and Astronautics, Kyushu University

出版情報：九州大学工学紀要. 68 (4), pp.175-192, 2008-12. 九州大学大学院工学研究院
バージョン：
権利関係：

Memoirs of the Faculty of Engineering, Kyushu University, Vol.68, No.4, December 2008

An Experimental Study on the Improvement of Aerodynamic Characteristics of Lifting Body Configuration by Active Flow Control Method

by

Shigeki TSUCHIYA[*], Shigeru ASO[**] and Yasuhiro TANI[***]

(Received November 4, 2008)

Abstract

To improve the aerodynamic characteristics of Reusable Launch Vehicles (RLV), active flow control methods with blowing have been investigated. The testing model is lifting body configuration with rounded leading edge and sweepback angle of 70 degrees. For the active flow control, the blowing along the upper surface of lifting body was chosen. The experiments was conducted in transonic wind tunnel of ISAS (Institute of Space and Astronautical Science), JAXA (Japan Aerospace Exploration Agency). The measurements of aerodynamic forces, flow visualizations and static pressure were conducted. In the series of experiments the increase of lift coefficient at higher angle of attack and the decrease of drag coefficient at lower angle of attack were observed in some conditions of the location of blowing and the sweptback angle and direction of the nozzle for active flow control. As a result the increase of ratio of Lift to Drag is observed among wide range of angle of attack in those selected conditions.

Keywords: Lifting body, Reusable Launch Vehicle, Active flow control, Vortex core, Blowing

Nomenclature

C_D	= drag coefficient
C_L	= lift coefficient
C_{My}	= pitching moment coefficient
C_μ	= blowing momentum coefficient
C_p	= pressure coefficient
L/D	= lift to drag ratio
M_∞	= free stream Mach number
$\dot{m}_b$	= mass flow rate of blowing

[*] Graduate Student, Department of Aeronautics and Astronautics
[**] Professor, Department of Aeronautics and Astronautics
[***] Assistant Professor, Department of Aeronautics and Astronautics

V_b = blowing velocity
q_∞ = dynamic pressure of free stream
S_{ref} = reference area of testing model
Re = Reynolds number ($=U_\infty L/\nu$)
α = angle of attack
Λ_N = sweepback angle of the nozzle
x_b = blowing nozzle location
L = model length
ν = kinematic coefficient of viscosity

1. Introduction

Space transportation system is one of the most important infrastructures for space activities. Nowadays development of RLV is in progress. Low cost, improvement of reliability and safety are strongly required for the development of RLV. One of the most important problems is to increase high aerodynamic performances of RLV for low cost, high reliability and safety. High lift performance at low speed regime makes possible shorter landing distance and lower approaching speed. High lift-to-drag ratio performance allows wide cross range and long down range during landing process.

Therefore we have conducted our experimental study in order to find the flow conditions to realize high aerodynamic performances for RLV by using active flow control method. As RLV flies in the range between hypersonic to subsonic regions, it is the best way that a single configuration, which does not change the shape of the vehicles, could realize high aerodynamic performance in the whole flight regions. However it is too difficult to realize such a configuration at the present situation. Therefore, the active flow control method has been proposed by the present authors in order to improve aerodynamic characteristics of RLV.

Generally, configurations of RLV are categorized into two types. One is wing-body type vehicle (e.g. Space Shuttle) and the other is lifting-body type vehicle (e.g. X-33 or X-38). From the point of view of aerodynamic heating, the lifting body configuration has much advantage because of rounded leading edge of body. On the contrary, the lack of main wing and the round leading edge of lifting-body configuration cause smaller lift compared with wing-body configuration. The wing-body configuration has good aerodynamic performance in subsonic and transonic regions.

In our laboratory, we have been studying about the aerodynamic characteristics of lifting body and wing body configurations[1)-3)]. In those studies, the detailed data of aerodynamic characteristics of RLV have been obtained. The selection of configurations of lifting-body or wing-body should be conducted based on the constraint and purpose of RLV. Therefore it is important to investigate the methods to increase aerodynamic performance of lifting-body for future possible missions. The purpose of the present study is to obtain high aerodynamic characteristics of lifting body configuration in subsonic region.

There are many mechanical devices for the improvement of aerodynamic characteristics, such as leading flaps and trailing flaps. And they have already been used practically. However those mechanical devices generate local high aerodynamic heating in hypersonic region. Therefore we decided to choose the blowing methods in order to reduce aerodynamic heating. The blowing methods are categorized mainly by blowing direction, position and their concepts. Vortex core blowing[4)-6)], span wise blowing[7) 8)] and tangential leading edge blowing[9) 10)] have been reported to be obtained an increase of lift or control of rolling moment characteristics. Most such experiments have been conducted in order to reinforce the leading-edge separation vortex directly.

Also lateral blowing has been proposed and some promising results have been reported.[11-17] In the lateral blowing, it have been reported that the flow near the trailing edge is dammed and the pressure of lower surface of the wing increases and the flow over upper surface of the wing was accelerated and the lift was increased by lateral blowing. However, no studies by lateral blowing have been conducted on lifting body.

For the section of blowing methods for lifting body, the present authors think that the most important point is how we could reinforce the leading-edge separation vortex. In this context, the blowing from the upper surface of lifting body was chosen. The leading-edge separation vortex on lifting body is shown in **Fig. 1**. For the purpose of reinforcing this vortex, the blowing nozzle was attached between the attachment line and secondary separation line. The objectives of the present study are to find combinations of location and direction of blowing from upper surface of lifting body in order to increase aerodynamic performance of lifting body.

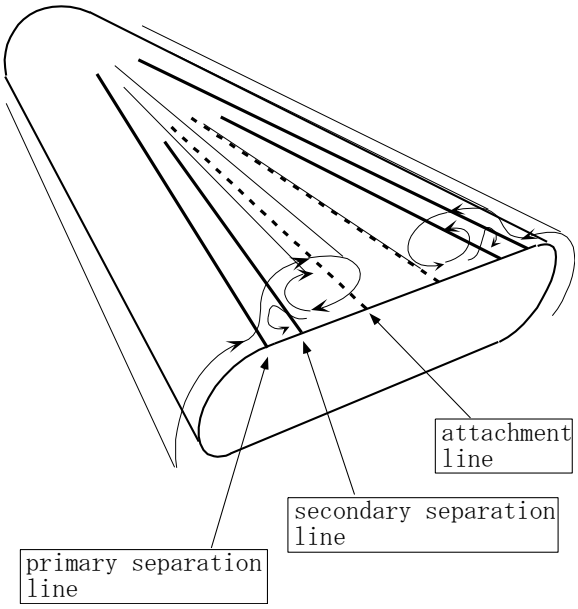

Fig. 1 Schematic of leading-edge separation vortex.

2. Experimental Apparatus and Procedures

2.1 Wind tunnel

The experiments were conducted in transonic wind tunnel of ISAS, JAXA. The wind tunnel is a blow-down type and has 600*mm*×600*mm* square test section. The wind tunnel has plenum chamber and porous wall at test section and is capable of Mach numbers sweep from 0.3 to 1.3.

2.2 Model and experimental apparatus

Figure 2 shows the testing model of lifting body configuration. The model length is 226.7*mm* and span width is 200*mm*. The radius of leading edge is 25*mm*, which is 12.5% of the width of the root span of the model. The reference area of the present study is $0.0265m^2$, which is the projection area of the top view of the lifting body. **Figure 3** shows the configuration of blowing nozzle and its location on upper surface of the model. The diameter of the nozzle is 2*mm* and the blowing is parallel to the upper surface of the model. The nozzle is detachable and the upper surface of the model can be flat. The locations of the nozzle are 30, 40, and 50% of the model length from the nose. And the sweepback angles of the blowing Λ_N are 50, 60 and 70*deg*. At no-blowing condition, the nozzle for blowing is not attached and the upper surface of the model is kept flat. At blowing condition, the nozzle is attached. The nozzle for blowing is located between the primary separation line and the secondary separation line. **Figure 3** also shows the location of static pressure holes. The location of static pressure holes are 70% of the model length from the nose. Total number of holes is 31.

The sting balance is used in the present study. The center of the balance is located at 165.7*mm* from the nose of the model and the location is used for reference moment center.

The experimental uncertainties measured at the calibration are about ±0.9% of full scale and each uncertainty is shown in each Figure.

2.3 Testing conditions

Testing conditions are shown in **Tables 1** and **2**. The aerodynamic forces of lift, drag and pitching moment are measured. The surface flow on the upper surface of the model is visualized by oil flow technique. The blowing momentum coefficient C_μ is used to evaluate the effect of the blowing. The blowing momentum coefficient is defined as shown in Eq. (1).

$$C_\mu = \frac{\dot{m}_b V_b}{q_\infty S_{ref}} \tag{1}$$

In the present study the value of C_μ is 0.0251 and is kept constant.

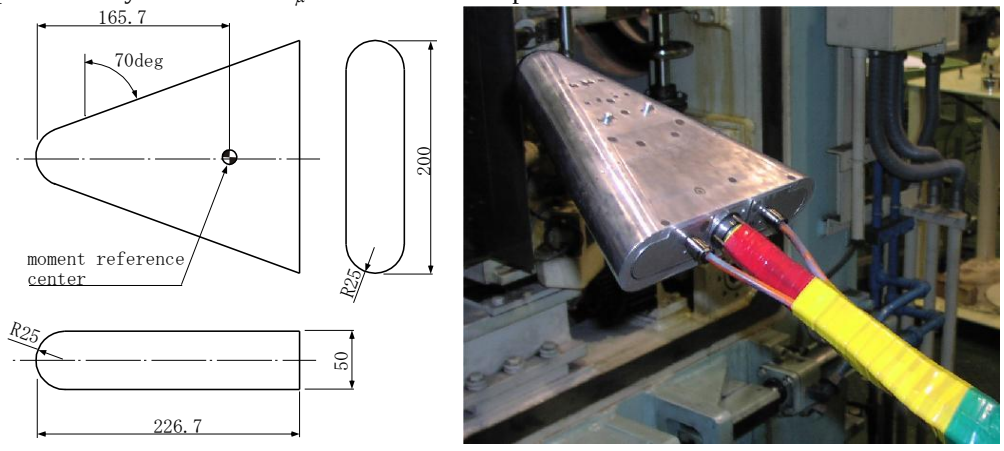

Fig. 2 Experimental model (unit: mm).

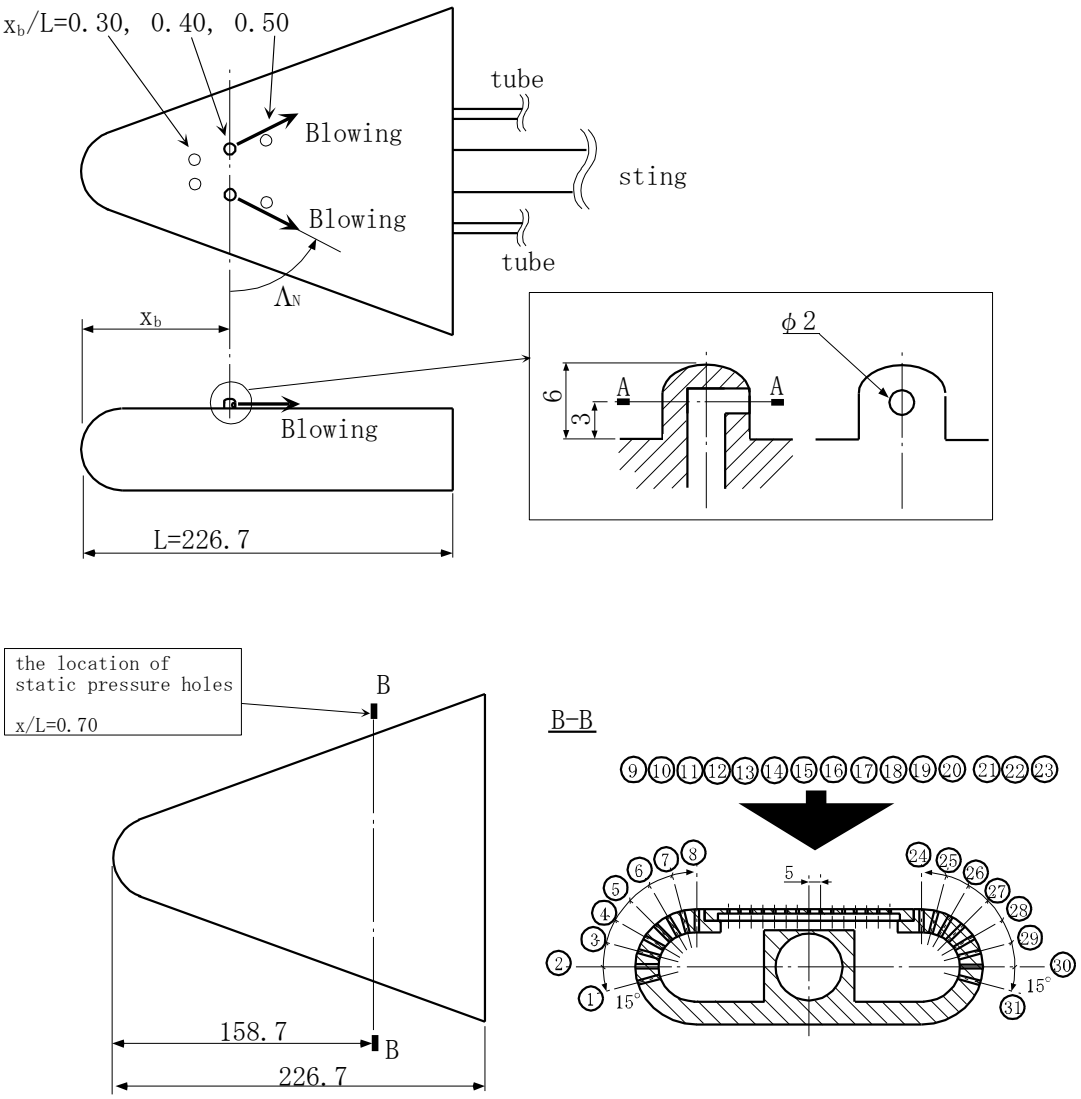

Fig. 3 Nozzle configuration and static pressure holes (unit: *mm*).

Table 1 Test conditions of aerodynamic measurement.

M_∞	C_μ	Re	α	x_b/L	Λ_N
0.3	0.0251	2.04×10^6	-15 ~ 40	0.3	50
0.3	0.0251	2.04×10^6	-15 ~ 40	0.3	60
0.3	0.0251	2.04×10^6	-15 ~ 40	0.3	70
0.3	0.0251	2.04×10^6	-15 ~ 40	0.4	50
0.3	0.0251	2.04×10^6	-15 ~ 40	0.4	60
0.3	0.0251	2.04×10^6	-15 ~ 40	0.4	70
0.3	0.0251	2.04×10^6	-15 ~ 40	0.5	50
0.3	0.0251	2.04×10^6	-15 ~ 40	0.5	60
0.3	0.0251	2.04×10^6	-15 ~ 40	0.5	70

Table 2 Test conditions of flow visualization and pressure measurement.

M_∞	C_μ	Re	α	x_b/L	Λ_N
0.3	0.0251	2.04×10^6	20, 30, 40	0.5	50

3. Results and Discussion

3.1 Aerodynamic forces of the model

The changes of C_L with respect to the angle of attack are shown in **Figs. 4~6**. The error bar of the data is shown at α=40degrees of the curve of model-only. In all the blowing conditions, the lift coefficient, C_L, increases at higher angle of attack. On the other hand, lift coefficient is almost same at lower angle of attack. The testing model does not show stall up to angle of attack of 40 *degrees*. The maximum lift coefficient is obtained at the condition of 40*degrees*. The value of maximum lift coefficient is 1.03 at the no-blowing condition and is 1.12 at blowing condition, where x_b/L *is* 0.40 and Λ_N is 50*deg*.

The changes of C_D with respect to the angle of attack are shown in **Figs. 7~9**. The error bar of the data is shown at α=40degrees of the curve of model-only. In all the blowing condition, the drag coefficient decreases near the condition of 0*deg* of angle of attack and increases above specific angle of attack. In **Fig. 7** (x_b/L=0.30), the drag coefficient similarly decreases below 25~30 degrees. On the other hand, it increases above 25~30 degrees. In **Fig. 8** (x_b/L=0.40), the drag coefficient shows almost same value between blowing and no-blowing cases at low angle of attack. Above angle of attack of 20 degrees, the drag coefficient significantly increases. In **Fig. 9** (x_b/L=0.50), the drag coefficient decrease due to blowing in almost all conditions. The minimum value of drag coefficient is 0.16 at the blowing condition (x_b/L=0.50, Λ_N=70*deg*) at angle of attack of 0 degrees. On the contrary the minimum value of drag coefficient is 0.18 at angle of attack of 0 degrees at no-blowing condition. The reduction of drag of 11% is obtained due to blowing at angle of attack of 0 degrees. As the direction of blowing is parallel to the upper surface of the body and is against the drag, the drag coefficient at low angle of attack is decreased significantly. Another possible reason of the reduction of drag is the acceleration of the flow in the center of the upper surface. The representative pictures of flow visualization by oil-flow technique at angle of attack of 20 degrees are shown in **Figs. 19** and **20**. Narrow and straight oil-flow lines are observed at the center of upper surface of the model at blowing condition. Those oil-flow lines indicate that the pressure around the center of the upper surface of the model decreases and the flow is accelerated due to large negative pressure caused by blowing.

The changes of pitching moment coefficient with respect to the angle of attack are shown in **Figs. 10~12**. The error bar of the data is shown at α=40degrees of the curve of model-only. In those figures almost no differences of pitching moment coefficients are observed between blowing and no-blowing conditions. In some cases the pitching moment coefficients increase slightly at higher angle of attack due to blowing.

The changes of lift to drag ratio with respect to the angle of attack are shown in **Figs. 13~15**. The error bar of the data is shown at α=40degrees of the curve of model-only. In **Fig. 13** (x_b/L =0.30), the value of lift to drag ratio with blowing shows higher value compared with no-blowing at x_b/L of 0.30 and Λ_N of 50 *deg*. In **Fig. 15** (x_b/L =0.50), lift to drag ratio significantly increases in all conditions. The maximum lift to drag ratio at no-blowing condition is 2.19 at the condition of 20*degs* of angle of attack. And the maximum lift to drag ratio at blowing condition is 2.64 at the condition of 17.5*deg* of angle of attack (x_b/L =0.40, Λ_N=70*deg*). In all blowing location case, the value of lift to drag ratio at Λ_N=70*deg* is larger than that of Λ_N=50*deg.*

When we focus on the lift coefficient, the comparisons of the efficiency of lift are shown in **Figs. 16~18**. The error bar of the data is shown at α=40degrees of the curve of x_b/L =0.30, Λ_N=50*deg*. The blowing is not efficient below the angle of attack of 22.5degrees, because dC_L/C_μ is less than 1. However, dC_L/C_μ shows more than unity, it can be said that the blowing is effective

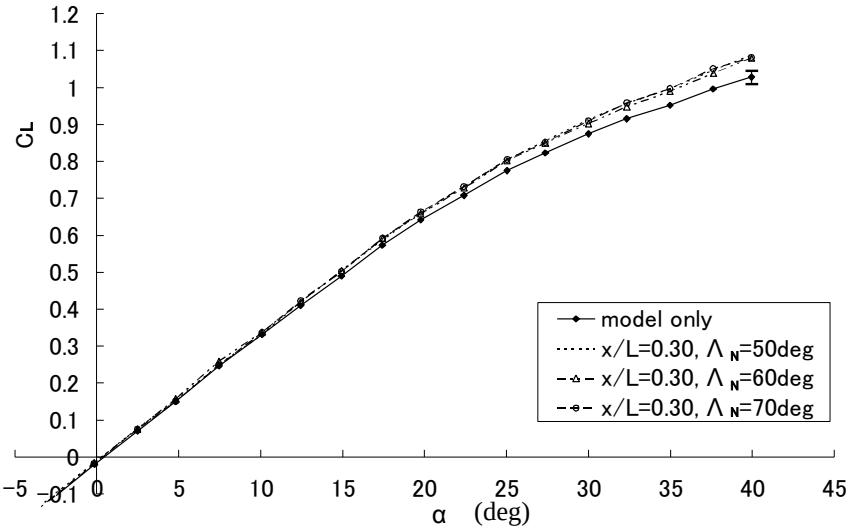

Fig. 4 Lift coefficient (x_b/L =0.30).

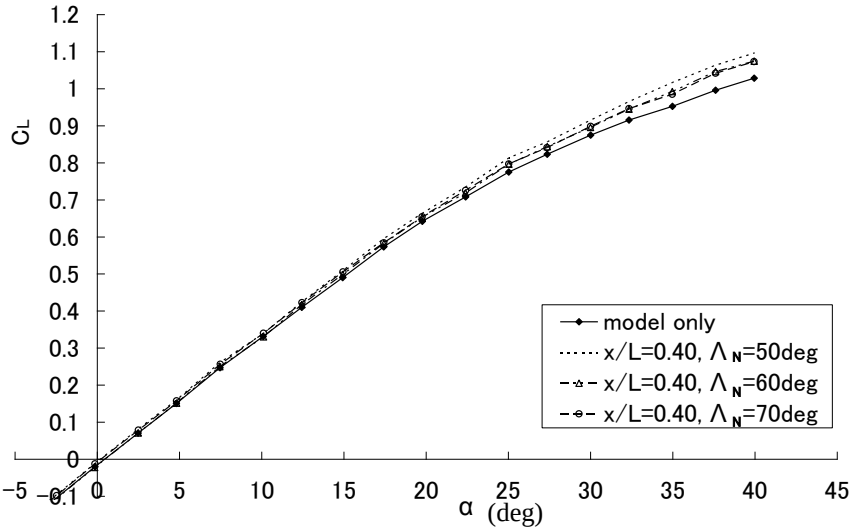

Fig. 5 Lift coefficient (x_b/L =0.40).

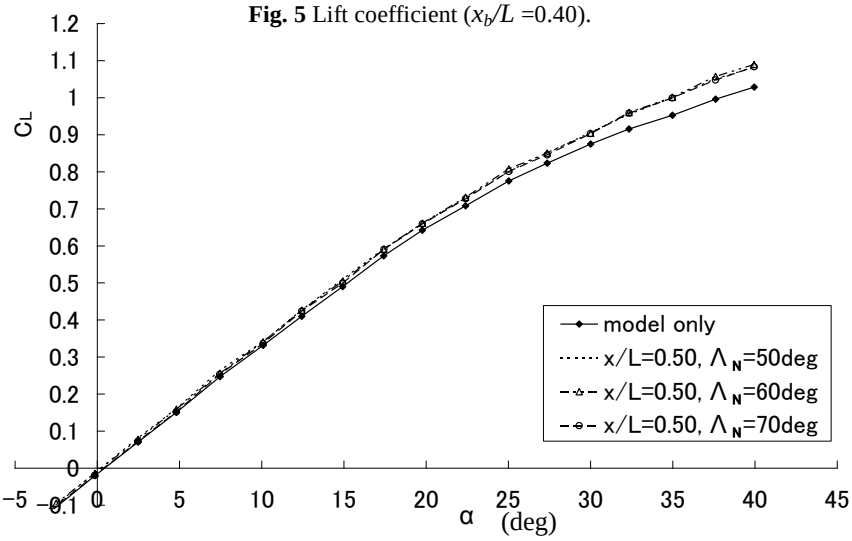

Fig. 6 Lift coefficient (x_b/L=0.50).

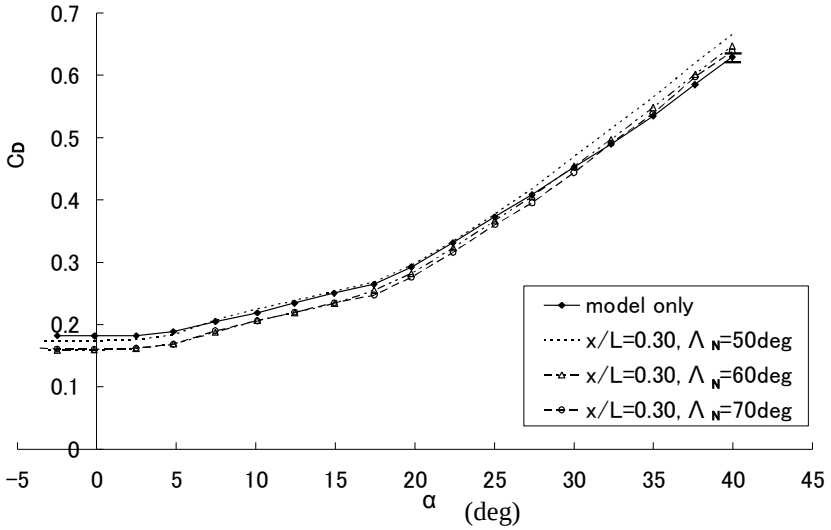

Fig. 7 Drag coefficient (x_b/L=0.30).

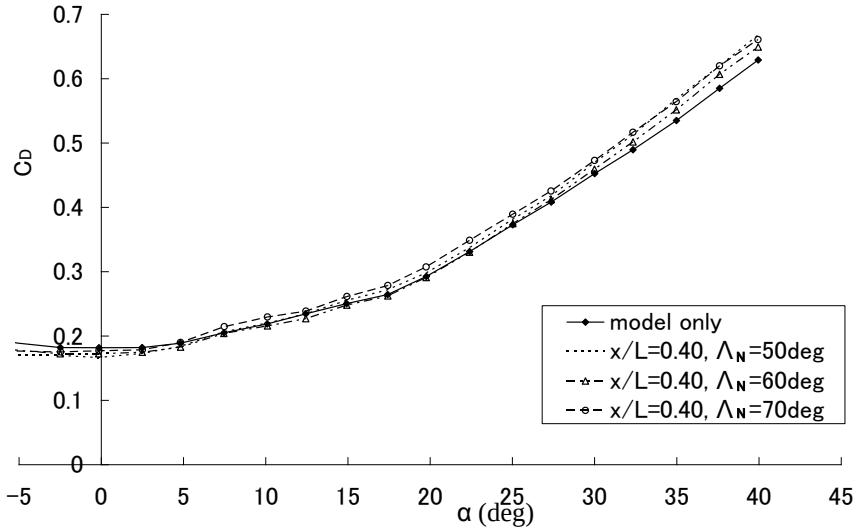

Fig. 8 Drag coefficient (x_b/L=0.40).

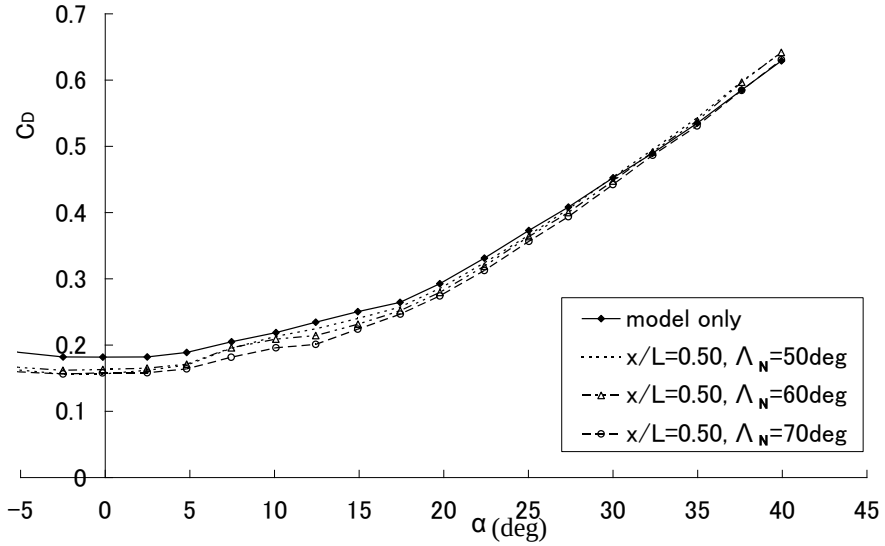

Fig. 9 Drag coefficient (x_b/L=0.50).

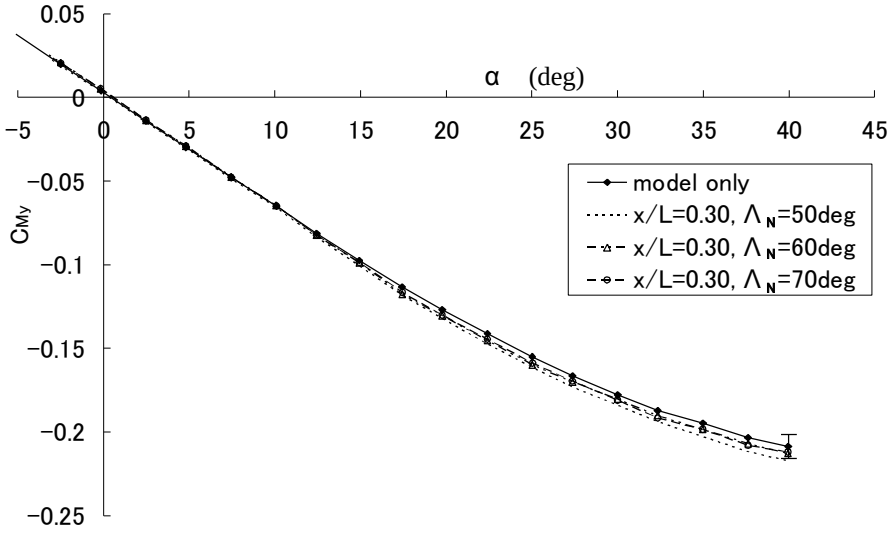

Fig. 10 Pitching moment coefficient (x_b/L=0.30).

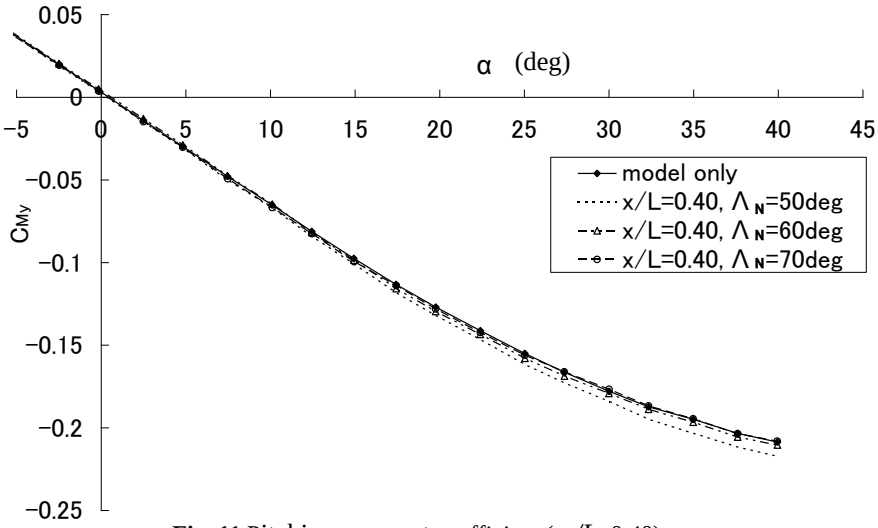

Fig. 11 Pitching moment coefficient (x_b/L=0.40).

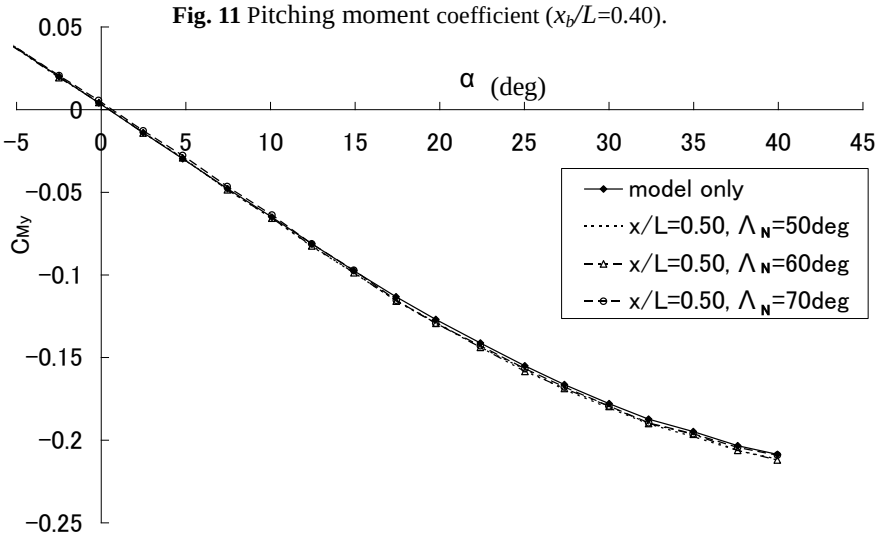

Fig. 12 Pitching moment coefficient (x_b/L=0.50).

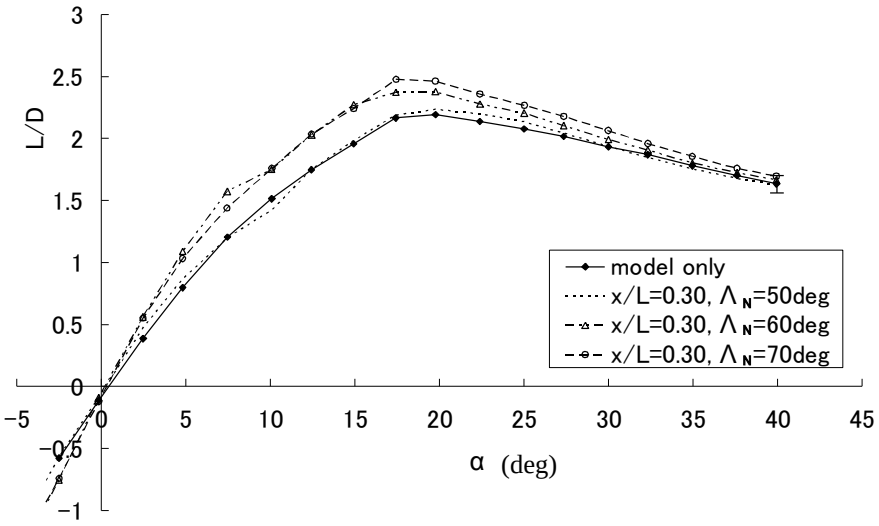

Fig. 13 Lift to Drag ratio (x_b/L=0.30).

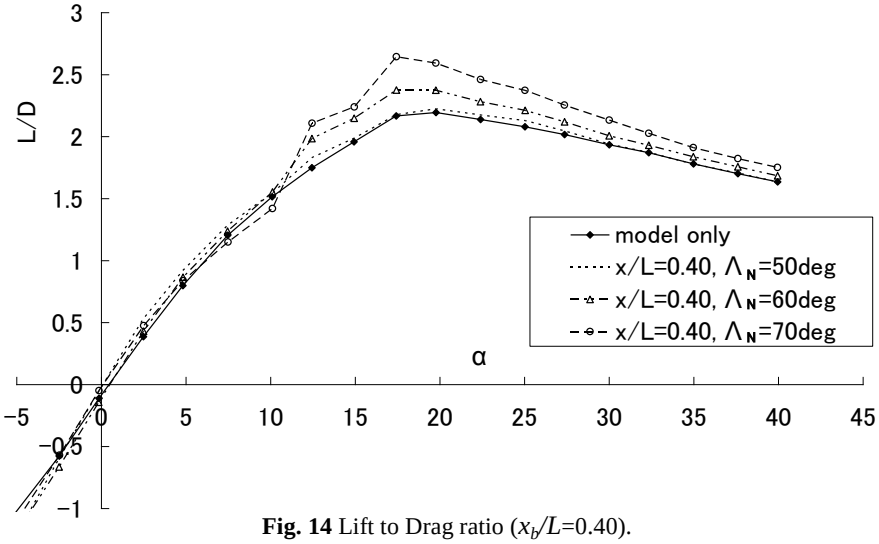

Fig. 14 Lift to Drag ratio (x_b/L=0.40).

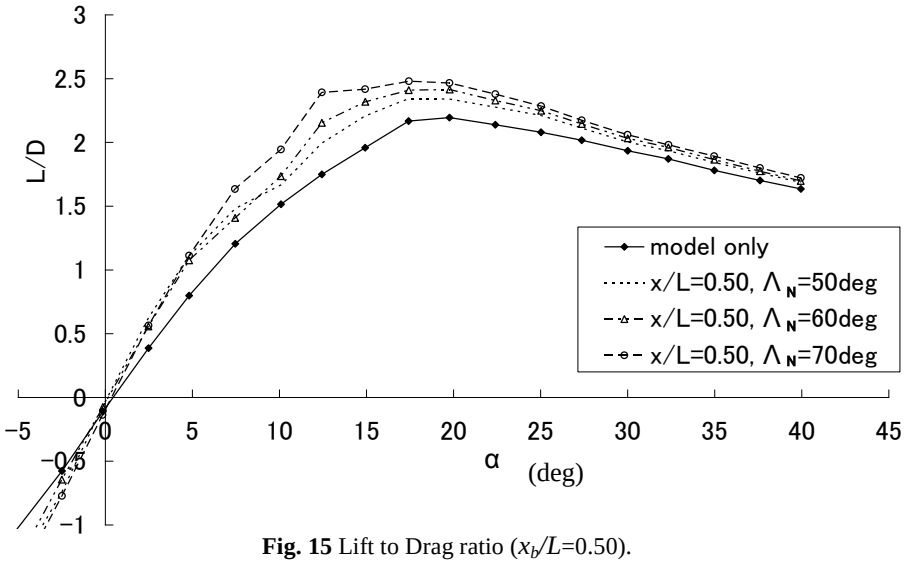

Fig. 15 Lift to Drag ratio (x_b/L=0.50).

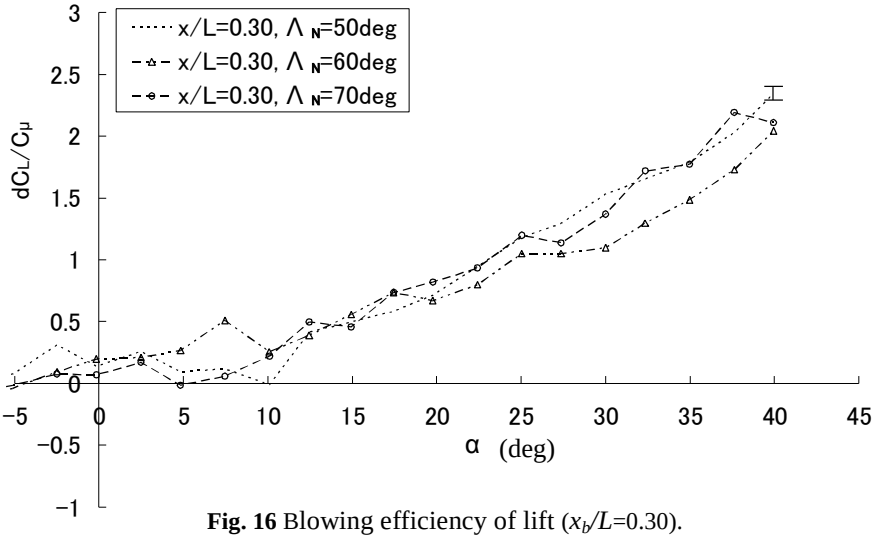

Fig. 16 Blowing efficiency of lift (x_b/L=0.30).

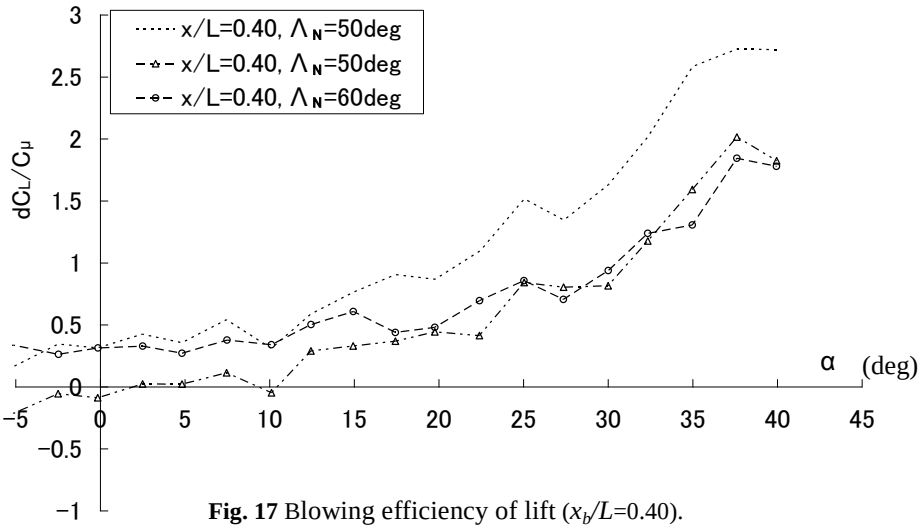

Fig. 17 Blowing efficiency of lift (x_b/L=0.40).

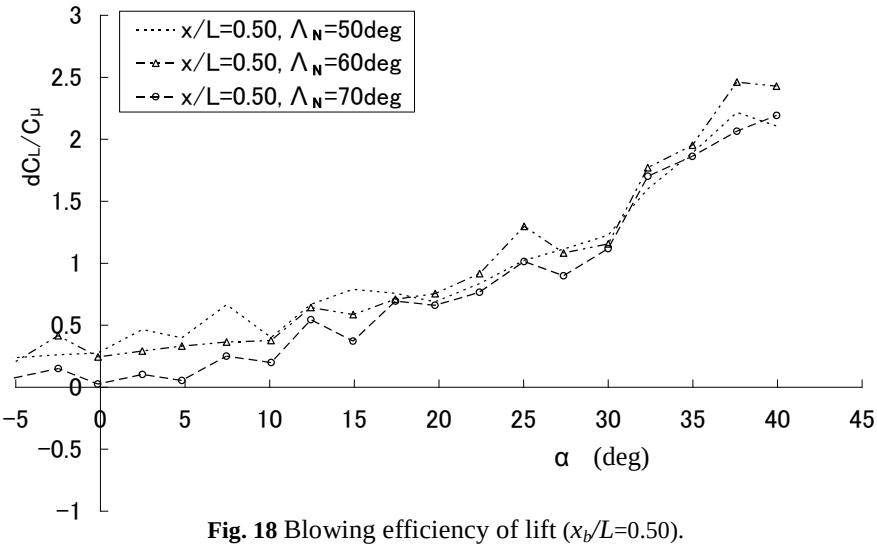

Fig. 18 Blowing efficiency of lift (x_b/L=0.50).

for the higher angle of attack. The most efficient case of this blowing is at the condition of x_b/L =0.40, Λ_N=50*deg.* And the value of dC_L/C_μ is 2.73 at the condition of 37.5degrees of angle of attack.

3.2 Flow visualization

Flow visualization results with oil flow technique are shown in **Figs. 19~24**. The cross sectional flow patterns at x/L=0.70 are also shown in the figures. The point a, b and c mean as

a: primary separation line
b: secondary separation line
c: attachment line

The nozzle is attached at the blowing condition and the blowing location is x_b/L =0.50, Λ_N=50*deg.* As shown in **Figs. 20**, **22** and **24**, the nozzle for blowing is located between the primary separation line and secondary separation line.

The results for the angle of attack of 20degrees are shown in **Figs. 19** and **20**. As shown in **Fig. 20**, the primary separation line of blowing condition moves to the leading edge of the body. This is because the jet flow through blowing nozzle pushes back the primary separation line upstream. The primary attachment line of blowing condition moves near the center line of the model compared with that of no-blowing condition. This is because the blowing increases the strength of leading edge vortex. Also the secondary separation line moves to the leading edge of the body. It is expected that the vortex on the lifting body is enlarged by the blowing. Therefore the pressure under the vortex is reduced and lift coefficient at the condition of 20degrees is increased by blowing as shown in **Fig. 6**.

The same flow patterns are observed at the condition of angles of attack of 30 and 40 *degrees*.

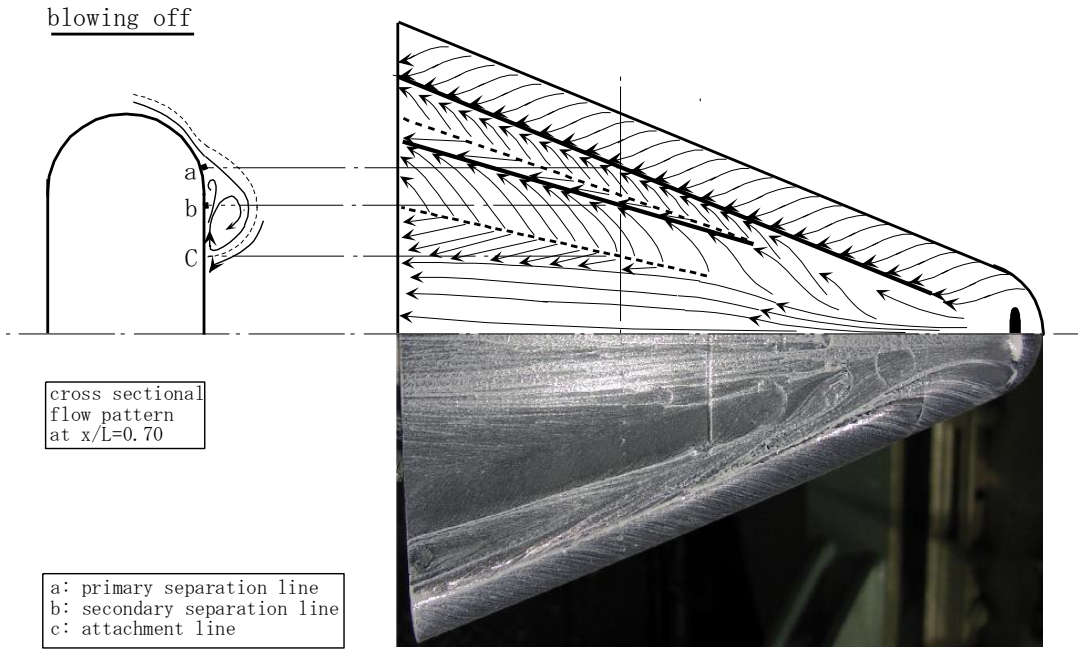

Fig. 19 Flow visualization (α=20deg, blowing off).

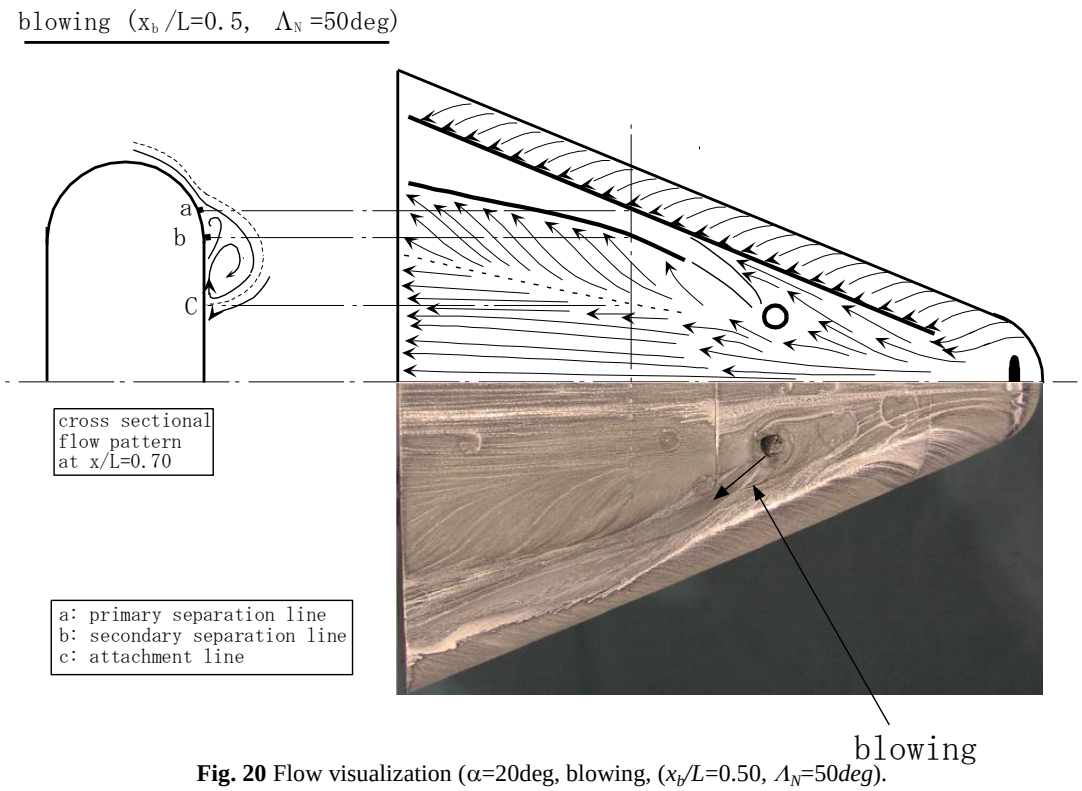

Fig. 20 Flow visualization (α=20deg, blowing, (x_b/L=0.50, Λ_N=50*deg*).

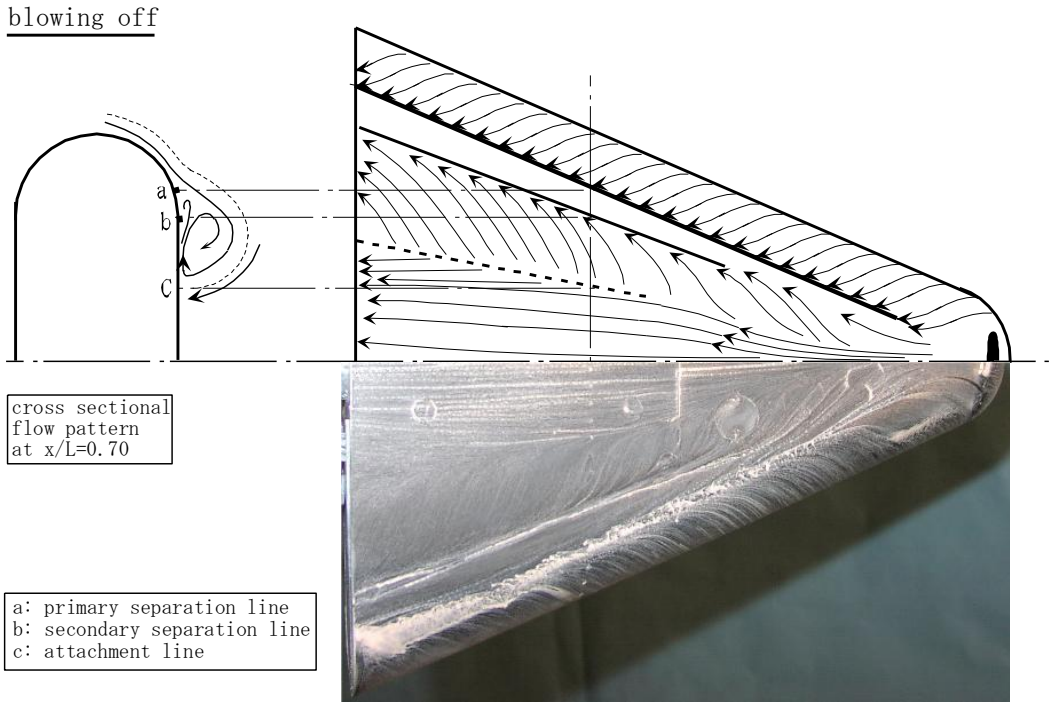

Fig. 21 Flow visualization (α=30deg, blowing off).

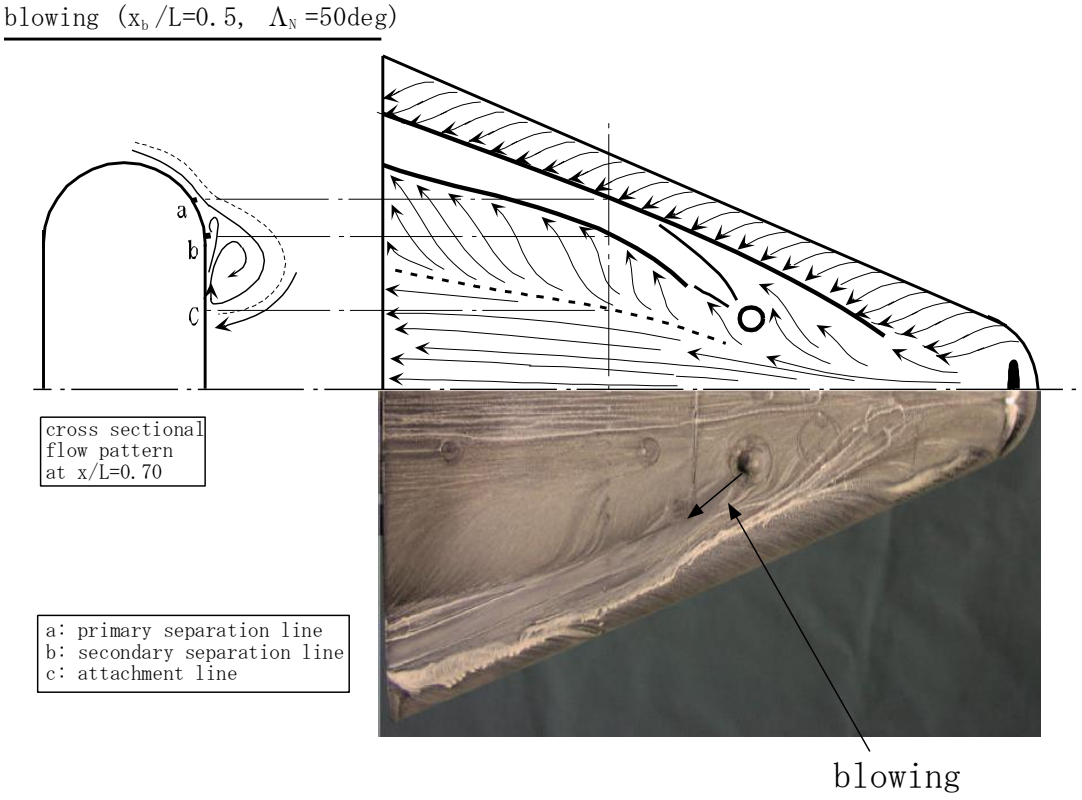

Fig. 22 Flow visualization (α=30deg, blowing, (x_b/L=0.50, Λ_N=50*deg*).

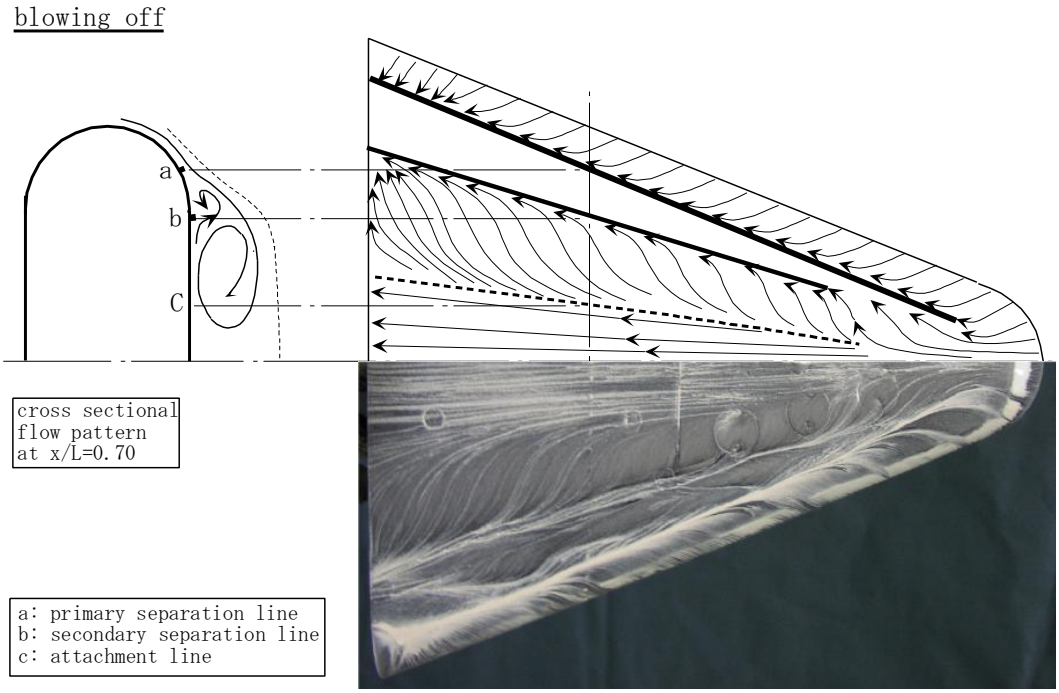

Fig. 23 Flow visualization (α=40deg, blowing off).

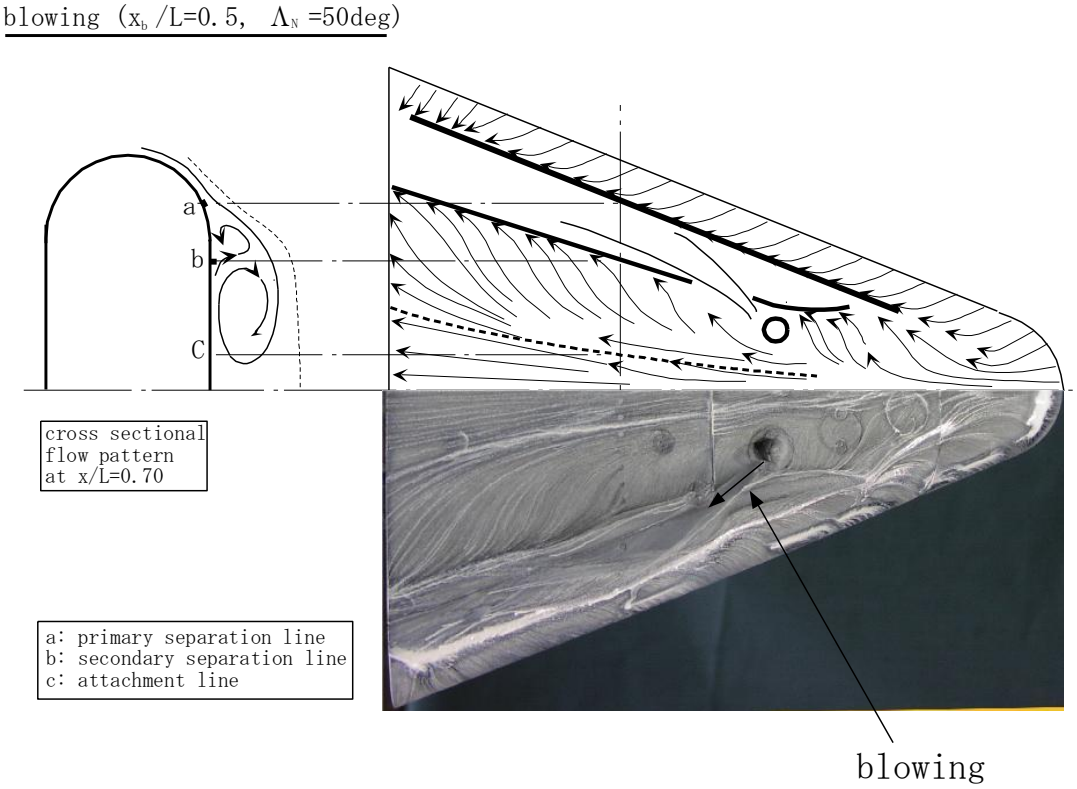

Fig. 24 Flow visualization (α=40deg, blowing, (x_b/L=0.50, Λ_N=50*deg*).

3.3 Static pressure results

The static pressure distributions at no-blowing condition and blowing condition of x_b/L =0.50 and Λ_N=50*deg* are shown in **Figs. 25** and **26**. The error bar of the data is shown at the location of 31 of the curve of no-blowing. Both Figures show negative pressure increase at location numbers of 9 and 23 because of the increase of strength of leading edge separation vortex. The numbers of 9 and 23 indicate the location of inner side of secondary separation line. Also the location is under the leading edge separation vortex whose strength is increased due to blowing. The increase of negative pressure near center line of upper surface of the body at blowing conditions is caused by the flow acceleration due to the blowing.

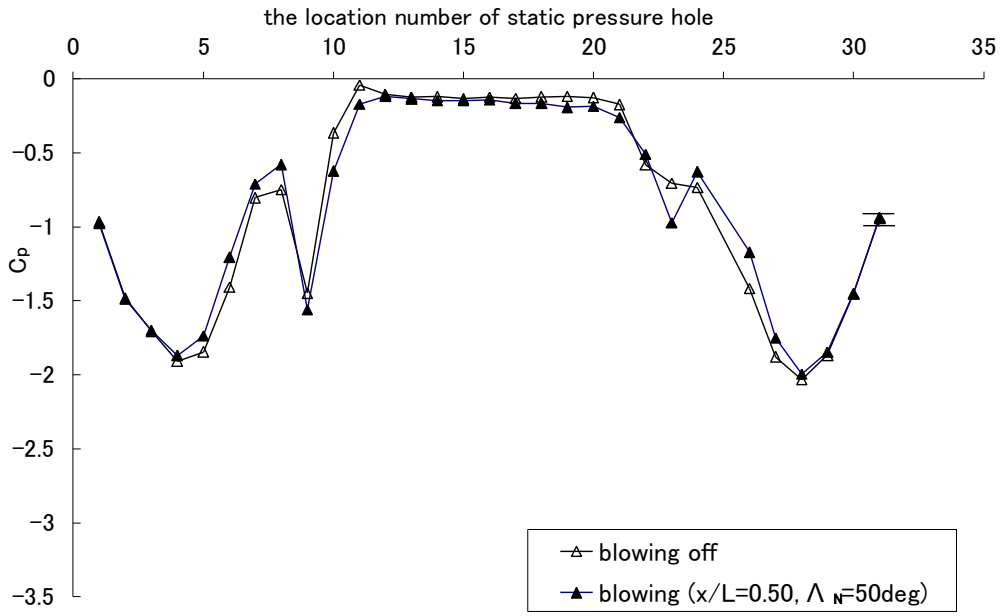

Fig. 25 Pressure distribution (α=30deg).

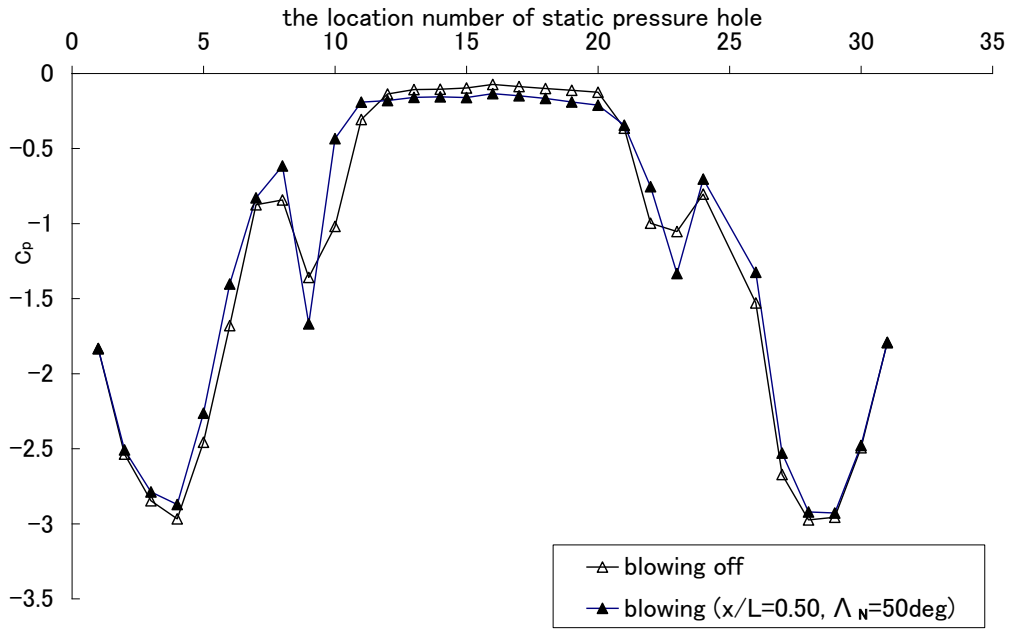

Fig. 26 Pressure distribution (α=40deg).

4. Conclusions

An experimental study on the improvement of aerodynamic characteristics of lifting body configuration by active flow control method was conducted in subsonic flow regions. The conclusions of the present study are summarized as follows:

(1) Lift coefficient increases at high angle of attack in all blowing conditions. And the value of maximum lift coefficient is 1.03 at the blowing-off condition and is 1.12 at blowing condition (x_b/L=0.40, Λ_N=50*deg*). The maximum lift coefficient increases about 10% by the blowing.
(2) Drag coefficient decreases near the condition of lower angle of attack and increase above higher angle of attack in all blowing conditions.
(3) Almost no differences of pitching moment coefficients are observed between blowing and no-blowing conditions. In some cases the pitching moment coefficients increase slightly at higher angle of attack due to blowing.
(4) The increase of lift coefficient at higher angle of attack and the decrease of drag coefficient at lower angle of attack are observed in some conditions of the location of blowing and the sweptback angle and direction of the nozzle for active flow control. As a result the increases of the ratio of Lift to Drag are observed among wide range of angle of attack in those selected conditions.
(5) The primary separation line of blowing condition moves to the leading edge of the body. This is because the jet flow through blowing nozzle pushes back the primary separation line upstream. The primary attachment line of blowing condition moves near the center line of the model compared with that of no-blowing condition. This is because the blowing increases the strength of leading edge vortex. Also the secondary separation line moves to the leading edge of the body. Therefore the pressure under the vortex is reduced and lift coefficient is increased by blowing.
(6) In the pressure distributions, the increase of negative pressure is observed at the location of inner side of secondary separation line because of the increase of strength of leading edge separation vortex. The increase of negative pressure near center line of upper surface of the body at blowing conditions is caused by the flow acceleration due to the blowing.

References

1) S. ASO, M. TSUJITA, S. TSUCHIYA, K. SATO and Y, KOBAYASHI : A Study on Lifting Body Aerodynamic Characteristics for Fully Reusable Launch Vehicle, 52nd International Astronautical Congress , 1-5 Oct 2001, IAF-01-V.3.07.
2) S. ASO, S. TSUCHIYA, M. TSUJITA, T. YONEDA, Y. KOBAYASHI and K. SATO : A Study on Aerodynamic Characteristics of Fundamental Configurations for Future Space Transportation Systems, 23rd International Symposium on Space Technology and Science, May 26-June 2, 2002, ISTS 2002-e−36.
3) Shigeru ASO, Yasuhiro TANI, Shigeki TSUCHIYA, Tomohisa YONEDA : A Study on Aerodynamic Characteristics of Lifting Body and Wing Body Configurations for Fully Reusable Launch Vehicles, 34th AIAA Fluid Dynamics Conference and Exhibit, AIAA-2004-2536.
4) James F. Campbell : Augmentation of Vortex Lift by Spanwise Blowing : J. Aircraft, Vol.13, No.9, SEPTEMBER 1976.

5) R. G. Bradley and W. O. Wray：A Conceptual Study of Leading-Edge-Vortex Enhancement by Blowing：J. Aircraft, Vol.11, No.1, JANUARY 1974.
6) R. G. Bradley, P. D. Whitten and W. O. Wray：Leding-Edge Vortex Augmentation in Compressible Flow：AIAA Paper No.75-124,1975.
7) Dhanvada M. Rao：Recent Studies of Slot-Blowing Techniques for Vortex Control on Slender Configurations：Fluid Dynamics on High Angle of Attack(IUTAM SYMPOSIUM TOKYO/JAPAN 1992), Springer-Verlag, pp.237-252.
8) John S.Hong, Zeki Z.Celik and Leonard Roberts：Effect of Leading-Edge Lateral Blowing on Delta Wing Aerodynamics：AIAA J., Vol.34, No.12, 1996, pp.2471-2478.
9) W. Gu, O. Robinson and D. Rockwell：Control of Vortices on a Delta Wing by Leading-Edge Injection：AIAA J., Vol.31, No.7, July 1993.
10) G.S.Wong, S.M.Rock, N.J.Wood and L.Roberts：Active Control of Wing Rock Using Tangential Leading-Edge Blowing：J. AIRCRAFT, Vol.31, No.3, 1994, pp.659-665.
11) Chiang Shih and Zhong Ding：Trailing-Edge Jet Control of Leading-Edge Vortices of a Delta Wing：AIAA J.,Vol.34,No.7, 1996, pp.1447-1457.
12) Karashima, K., “Augmentation of Aerodynamic Performance of Low Aspect-Ratio Wings by Use of a Lateral Blowing at the Trailing Edge,” The 28th Fluid Dynamics Conferences, JSASS, Japan, 1996, pp. s-17-s-26.
13) Kamishita, M., and Aso, S., “A Study on Improvement of Aerodynamic Characteristics of the Next-Generation SST Wing by Lateral Blowing in Subsonic Flow,” Journal of The Japan Society for Aeronautical and Space Sciences, Vol. 49, No. 569, 2001, pp. 174-180.
14) Aso, S., Kamishita, M., Karashima, K., and Sato. K., “A Study on Active Flow Control for Next-Generation SST for Higher L/D,” AIAA Paper 2002-2844, Jun. 2002.
15) Kamishita, M., Aso, S., Karashima, K., and Sato. K., “Improvement of Aerodynamic Characteristics of Next-Generation SST Wing by Lateral Blowing,” Proceedings of 22nd International Congress of Aeronautical Sciences, Sep. 2000.
16) Miyaji, K., Fujii, K., and Karashima, K., “Enhancement of the Leading-Edge Separation Vortices by Trailing-Edge Lateral Blowing,” AIAA Journal, Vol. 34, No. 9, 1996, pp. 1943-1945.
17) Tadakuma, K., Aso, S., and Tani, Y., “Active Control of Aerodynamic Characteristics of Space Transportation System by Lateral Blowing,” AIAA Paper 2004-2718, Jun. 2004.